Cross sections for photoionization of fullerene molecular ions C_n^+ with $n = 40$, 50, 70, 76, 78, and 84

C. M. Thomas,[1] K. K. Baral,[1] N. B. Aryal,[1] M. Habibi,[1] D. A. Esteves-Macaluso,[1,*] A. L. D. Kilcoyne,[2] A. Aguilar,[2] A. S. Schlachter,[2] S. Schippers,[3,4] A. Müller,[3] and R. A. Phaneuf[1,†]

[1]*Department of Physics, University of Nevada, Reno, Nevada 89557-0220, USA*

[2]*Advanced Light Source, MS 7-100, Lawrence Berkeley National Laboratory, Berkeley, California 94720, USA*

[3]*Institut für Atom- und Molekülphysik, Justus-Liebig-Universität-Giessen, D-35392 Giessen, Germany*

[4]*I. Physikalisches Institut, Justus-Liebig-Universität-Giessen, 35392 Giessen, Germany*

(Received 15 March 2017; published 22 May 2017)

Absolute cross-section measurements are reported for single photoionization of C_n^+ fullerene molecular ions ($n = 40$, 50, 70, 76, 78, and 84) in the photon-energy range 18–70 eV. The experiments were performed by merging a mass and charge selected beam of C_n^+ molecular ions with a beam of monochromatized synchrotron radiation and measuring the yield of C_n^{2+} product ions as a function of the photon energy. Oscillator strengths determined by integrating the measured cross sections over this energy range exhibit a linear dependence on n. The cross sections are parametrized by fits to three Lorentzian functions to represent plasmon excitations and a linear function for direct ionization. The highest-energy resonance in the data near 46 eV is similar to that previously observed in single photoionization of C_{60} and may be attributable to a harmonic of the dominant surface-plasmon resonance near 23 eV.

DOI: 10.1103/PhysRevA.95.053412

I. INTRODUCTION

The discovery of C_{60} in 1985 by Kroto and collaborators [1] has motivated numerous investigations of the unique properties of fullerene molecules during the ensuing three decades [2,3]. Fullerenes bridge the gap between free molecules and pure crystalline solids because of their nanometer size, hollow cage structures, homonuclearity, and symmetry, giving rise to novel phenomena. Among them are broad resonance features in the photoionization cross sections of C_{60} and C_{60}^+ that have been attributed to plasmon excitations of the delocalized valence electrons in the molecule [4–9]. Very recently, Hansen *et al.* [10] reported evidence of a Boltzmann distribution of electron velocities resulting from photionization of C_{60}, which they attribute to a quasithermal boiloff mechanism involving large numbers of incoherently excited valence electrons.

Their closed, empty-cage geometries permit stable fullerene molecules C_n to consist only of even numbers of C atoms with $n \geqslant 20$, consistent with Euler's theorem for closed polyhedrons [9]. Fullerenes have been detected by laser-desorption mass spectrometry in carbonacious sediments of meteor-impact craters with even carbon atom numbers ranging from 60 to 250 [11,12]. The relative abundances of fullerene molecules C_n are dependent upon n with maxima observed in their laboratory synthesis at 60, 70, 76, 78, and 84. Fullerene molecules with n less than 60 do not have long-term stability but their ions are readily produced by fragmentation of higher-n fullerenes in collisions [2] or by photoabsorption [13]. Fullerene molecules with $n \leqslant 60$ are spherical, but become progressively more prolate with increasing n greater than 60.

Absolute photoionization cross-section measurements for fullerene ions were first reported by Scully *et al.* [6] by merging mass-charge analyzed fullerene ion beams with a beam of tunable monochromatized synchrotron radiation. Cross sections for single photoionization of C_{60}^+, C_{60}^{2+}, and C_{60}^{3+} ions were measured over the photon-energy range 17–75 eV. In addition to the prominent surface-plasmon resonance near 22 eV predicted theoretically by Bertsch *et al.* [4] and first observed in photoionization of C_{60} by Hertel *et al.* [5], a second broad feature was identified near 38 eV that was attributed, on the basis of a theoretical calculation using the time-dependent local-density approximation (TDLDA), to a higher-order collective (volume) plasmon resonance [6–9]. A comparably strong surface-plasmon resonance near 22 eV was also observed in photoionization of C_{70} [5].

Absolute cross-section measurements have been recently reported by Baral *et al.* for 23 different fullerene ion products following photoexcitation of C_{60}^+ in the 18–150 eV photon-energy range [13]. The processes investigated include single and double photoionization, accompanied by the loss of 0–7 pairs of C atoms, as well as fragmentation without ionization of the fullerene resulting in the loss of 2–8 pairs of C atoms. On the basis of the Thomas-Reiche-Kuhn (TRK) oscillator-strength sum rule [14], an accounting of oscillator strengths indicated that production of a smaller fullerene ion occurs with nearly 50% probability following photoexcitation in this energy range. Very recently, Douix *et al.* reported measurements of cross sections for single photoionization of C_{60}^+ based on both the merged-beams and ion-trapping methods [15]. While their merged-beams results are in agreement with those of Baral *et al.*, the ion trap data are larger by nearly a factor of three near the peak of the cross section. Douix *et al.* attribute this difference to internal excitation of the C_{60}^+ ions produced in the discharges of the electron-cyclotron-resonance (ECR) ion sources that were used in both merged-beams experiments, even though they were operated at extremely low rf power. Their experiment thereby confirms speculation by Baral *et al.* about the likely role of internal excitation of C_{60}^+ leading to product channels involving ionization accompanied by fragmentation of the fullerene ion.

*Present address: Department of Physics and Astronomy, University of Montana, Missoula, MT 59812, USA.

†phaneuf@unr.edu

In the present paper, absolute cross-section measurements are reported for single photoionization of C_{40}^+, C_{50}^+, C_{70}^+, C_{76}^+, C_{78}^+, and C_{84}^+ over the photon-energy range 18–70 eV. Oscillator strengths are deduced from the measurements and their dependence on the number of carbon atoms in the molecular ion is examined.

II. EXPERIMENT

The measurements were performed at the ion photon beam (IPB) end station on undulator beamline 10.0.1.2 of the Advanced Light Source. Since the experimental setup and merged-beams method have been described previously [16,17], only a brief summary is given here with details specific to the current investigation.

C_n^+ ions were produced by evaporating commercially refined mixed heavy fullerene powder from a small resistively heated oven into a low-power Ar discharge within the plasma chamber of a permanent-magnet electron-cyclotron resonance ion source [18]. In the case of C_{84}^+ a sample of purified C_{84} was used. C_n^+ ions with $n \geqslant 60$ were produced by ionization of fullerene molecules evaporated into the plasma chamber, whereas C_{40}^+ and C_{50}^+ resulted from fragmentation and ionization of heavier fullerenes (mainly C_{60}) in the discharge. C_n^+ ions were extracted from the ion source, focused, collimated and mass analyzed prior to being electrostatically merged onto the axis of a counterpropagating beam of monochromatized synchrotron radiation. After a common path of approximately 1.4 m in ultrahigh vacuum, the ion beam was demerged from the photon beam by a dipole magnet. The magnet and a spherical electrostatic analyzer located immediately downstream deflected the product ion beam in orthogonal directions and selectively directed C_n^{2+} products to a channeltron-based single-particle detector [19]. The detection efficiency for 6 keV C_{60}^{2+} was measured *in situ* to be 0.79 ± 0.03 and was assumed to be the same for the other C_n^{2+} products. Four-jaw slits located in front of the detector permitted adjustment of the mass resolution and verification of complete separation and collection of C_n^{2+} product ions. The photon beam was mechanically chopped at 6 Hz to separate photoions from the same products resulting from collisions with residual gas in the ultrahigh vacuum system. The primary C_n^+ ion beam was simultaneously collected in a Faraday cup and its current measured by a precision electrometer. The photon beam was directed onto a calibrated Si x-ray photodiode[1] from which the photocurrent provided a measure of its absolute intensity at each selected photon energy.

To determine absolute cross sections at specific photon beam energies, the spatial overlap of the beams in a central electrostatically biased interaction region of length 29.4 ± 0.6 cm was quantified using three translating-slit scanners located near the beginning, middle, and end of the interaction region. The bias potential facilitated energy labeling of products from within that region where the spatial overlap of the two beams was accurately quantified.

The measurements were carried out in two stages. First, spectroscopic measurements were made by merging the photon and each of the C_n^+ ion beams and recording the normalized yield of C_n^{2+} ions for each as the photon beam energy was scanned in 0.5 eV steps over the energy range 18–70 eV. Because the monochromator slits were fixed during these scans, the photon-energy spread varied across this energy range, but was everywhere comparable to or smaller than the energy step size, which was typically 0.5 eV. The photon-energy resolution was considered unimportant because of the absence of narrow resonance features in the measured photoion-yield spectra.

The second stage involved performing absolute cross-section measurements for single ionization yielding C_n^{2+} products from C_n^+ under conditions in which the spatial overlap of the beams in the central interaction region was measured. These measurements were made for each n at fixed photon energies of 22, 35, 38, and 65 eV. The broad spectroscopic scans for the C_n^{2+} product ions were then placed on an absolute scale by normalizing them to these cross-section measurements. The presence of a small fraction of higher-order radiation in the photon beam produced by the undulator and dispersed by the monochromator was taken into account in the data analysis [20]. The total systematic uncertainty in the absolute measurements is estimated to be $\pm 24\%$. Statistical uncertainties of the data in the spectroscopic scans and absolute cross-section measurements are in all cases negligibly small in comparison.

III. RESULTS

Figure 1 presents a comparison of the cross-section measurements for single photoionization of C_{40}^+, C_{50}^+, C_{60}^+, C_{70}^+, C_{76}^+, C_{78}^+, and C_{84}^+ over the photon-energy range 18–70 eV. The results for C_{60}^+ are taken from Ref. [13]. The absolute cross-section measurements to which the spectroscopic scans are normalized are collected in Table I. The strong surface-plasmon resonance occurring near 23 eV is the dominant feature in each of the measured cross sections, which have similar dependences on photon energy. The second broader plasmon resonance occurring near 35 eV reported by Scully *et al.* [6] for C_{60}^+ at 38 eV is also evident, although there is some variation in the widths, energy positions, and relative strengths of this feature. With the exception of C_{40}^+, the measurements additionally show evidence for a third feature near 46 eV. These resonant features are discussed in detail in Sec. IV. An experimental estimate of the dimensionless oscillator strength may be determined by integrating the measured cross sections over an appropriate energy range as follows:

$$f = 9.11 \times 10^{-3} \int_{E_1}^{E_2} \sigma(E) dE, \tag{1}$$

where the photon energies E are in eV and the cross section σ is in Mb. Integrating each of the cross sections in Fig. 1 over the energy range 18–70 eV and applying Eq. (1) provides an experimental determination of the oscillator strengths as functions of the number of C atoms, n. The result is presented

[1]International Radiation Detectors model SXUV100-06-9 no. 35 referenced to SXUV100-07-8 no. 1 calibrated by NIST in 2008. The quantum efficiency of the working photodiode was compared periodically with that of a reference photodiode for changes due to radiation damage.

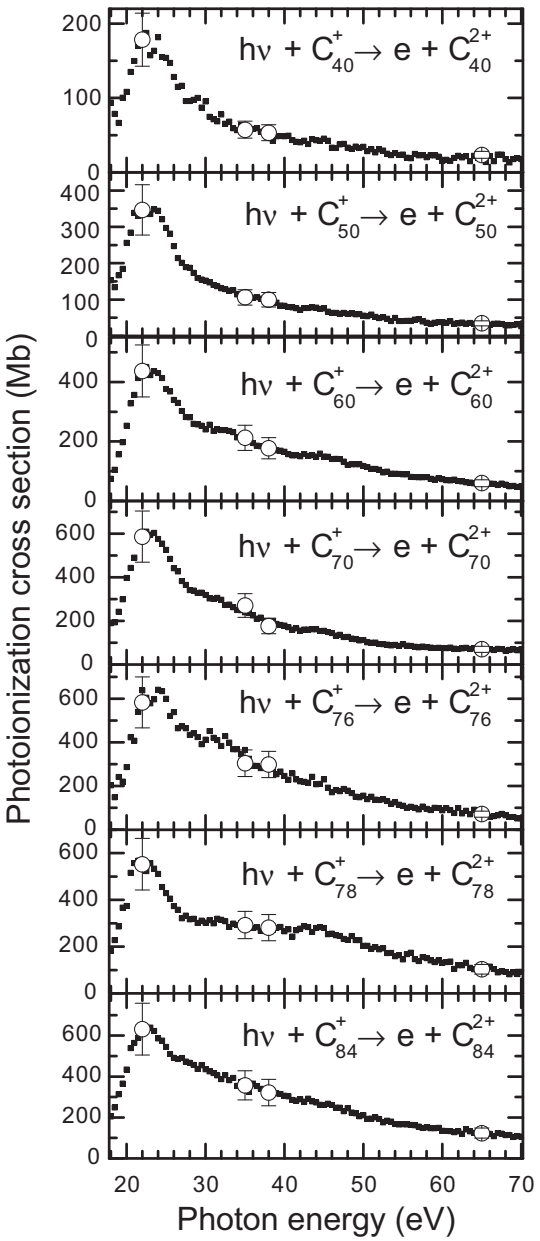

FIG. 1. Experimental results for single photoionization of C_n^+. Small solid squares represent energy-scan measurements and large solid circles with error bars are absolute cross-section measurements to which the scans are normalized. The C_{60}^+ data are taken from Ref. [13].

in Fig. 2, which shows a linear dependence of the oscillator strengths on n in this energy range.

IV. PARAMETRIZATION OF CROSS SECTIONS

Parametrizations of the photoionization cross sections were carried out in a manner similar to that reported by Scully *et al.* [6] for photoionization of C_{60}^+. Least-squares fits were made of the measured cross sections σ as functions of the photon energy E in terms of Lorentzian functions to represent plasmon excitations and a linear function decreasing slowly with photon energy to approximate a small contribution due

TABLE I. Measured absolute cross sections for single photoionization of C_n^+ molecular ions. Absolute uncertainties correspond to a one-sigma confidence level. The values for C_{60}^+ are taken from Ref. [13].

Primary ion	Photon energy (eV)	Cross section (Mb)	Absolute uncertainty (Mb)
C_{40}^+	22	178	36
	35	57.4	11.5
	38	53.3	10.7
	65	23.5	4.6
C_{50}^+	22	377	70
	35	106	21
	38	99.6	19.9
	65	34.8	6.9
C_{60}^+	22	425	98
	35	211	48
	38	177	35
	65	57.4	11.5
C_{70}^+	22	586	117
	35	271	54
	38	177	35
	65	70.0	14.1
C_{76}^+	22	583	117
	35	304	61
	38	299	59
	65	70.8	14.2
C_{78}^+	22	553	110
	35	292	59
	38	282	55
	65	103	21
C_{84}^+	22	632	126
	35	357	72
	38	321	64
	65	124	25

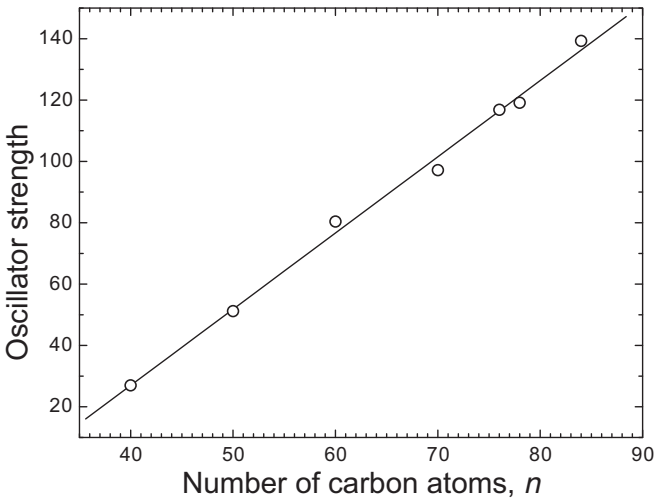

FIG. 2. Dimensionless oscillator strengths (open circles) determined by integrating the cross sections in Fig. 1 and applying Eq. (1). The line represents a linear least-squares fit to the data.

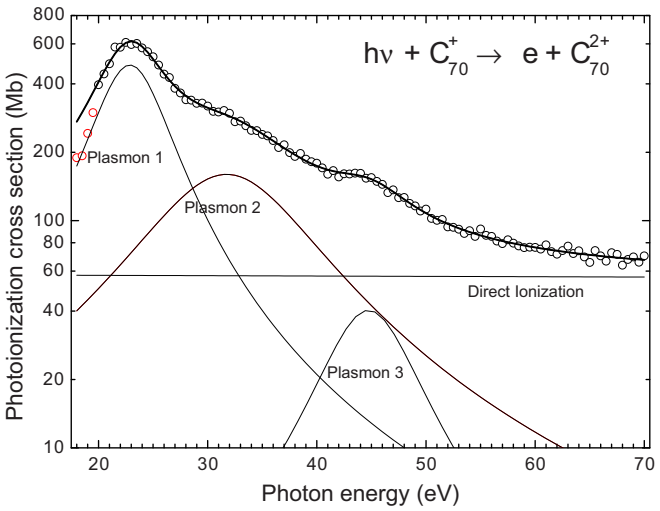

FIG. 3. Least-squares fit of a linear and three Lorentzian functions using Eq. (2) to the cross section for single photoionization of C_{70}^+. The four lowest-energy data points were excluded from the fitting procedure due to possible systematic effects in the recording of the photon flux.

to nonresonant photoionization as follows:

$$\sigma = mE + b + \sum_{i=1}^{3} \frac{2A_i}{\pi} \frac{\Gamma_i}{4(E - E_i)^2 + \Gamma_i^2}. \qquad (2)$$

In Eq. (2), m denotes the slope and b the intercept of the linear function representing direct photoionization. The parameters A_i, E_i, and Γ_i denote the area, photon energy, and energy full width at half maximum, respectively, of plasmon excitations. Two plasmons were included in the fitting of the cross section for photoionization of C_{60}^+ measured by Scully *et al.*, the first representing dipole excitation near 22 eV of a surface plasmon due to a symmetric in-phase oscillation of the delocalized electrons on the inner and outer surfaces of the spherical electron shell, resulting in no localized variations of electron density within the shell. A second broader resonance feature was identified near 38 eV. On the basis of the time-dependent local density approximation, this feature was attributed to an antisymmetric plasmon mode in which the oscillations of the electrons on the inner and outer surfaces of the electron shell are out of phase. The labeling of this resonance feature as a volume plasmon proved to be somewhat controversial [7,8].

The present measurements additionally show evidence for a third resonance feature near 46 eV that is interpreted as a harmonic of the surface-plasmon resonance, as discussed below. This feature was not evident in the data of Scully *et al.* for C_{60}^+. Its resolution in the present measurements and that of Baral *et al.* for C_{60}^+ is attributed to numerous subsequent improvements to the IPB end station, as discussed in detail by Baral *et al.* [13]. These included operation of the ECR ion source at lower rf power to reduce internal excitation of the fullerene ions, an improved x-ray photodiode resistant to changes in calibration, a photoion detector with increased mass resolution, and correction of the data for the effect of a small fraction (a few percent) of higher-order radiation from the undulator.

In measurements of single photoionization of neutral C_{60}, three resonant features were also reported by Kou *et al.* [21,22] and subsequently by Kafle *et al.* [23] at photon energies near 26 eV, 34 eV, and between 40 and 50 eV. They speculated that the two higher-energy features might be attributable to a shape resonance in photoionization of the C_{60} valence shell whereby the ionized electron is temporarily trapped inside a strong centrifugal barrier. Regardless of their physical origins, the resonant features observed in photoionization of C_n^+ ions are hereafter in this paper referred to as the first, second, and third plasmons.

Three Lorentzian functions were included in the fitting procedure, resulting in satisfactory representations of the energy dependences of the present cross-section measurements for the C_n^+ ions investigated and for that measured by Baral *et al.* for C_{60}^+. Figure 3 shows the results for C_{70}^+ as a representative example of the quality of the fits and indicates the relative contributions of each of the terms in Eq. (2). The third resonant feature with a relatively small amplitude near 46 eV is evident in the data. The fitting parameters for all the reported cross sections are collected in Table II. It should be noted that the fits apply to the cross sections in the photon-energy range 20–70 eV only and are not expected to give reliable estimates of the cross sections outside this range.

The fitted values for the photon energy of the first plasmon are similar for all the ions, with a mean value of 22.7 ± 0.4 eV. For C_{60}^+, the current value of 23.0 ± 0.06 eV compares

TABLE II. Fitting parameters of the cross sections for single photoionization of C_n^+ and their uncertainties.

Parameter	C_{40}^+	C_{50}^+	C_{60}^+	C_{70}^+	C_{76}^+	C_{78}^+	C_{84}^+
m (Mb/eV)	-0.10 ± 0.10	-0.31 ± 0.02	-0.18 ± 0.02	-0.02 ± 0.02	-0.19 ± 0.04	-0.09 ± 0.03	-0.12 ± 0.02
b (Mb)	16.8 ± 4.5	45.2 ± 2.4	51.3 ± 4.5	57.9 ± 1.9	61.9 ± 9.7	77.4 ± 8.2	84.2 ± 7.9
A_1 (Mb*eV)	1612 ± 359	4101 ± 248	4012 ± 315	5554 ± 264	4417 ± 835	4030 ± 734	3690 ± 930
Γ_1 (eV)	7.73 ± 0.87	8.72 ± 0.35	7.32 ± 0.35	7.30 ± 0.21	6.40 ± 0.66	6.39 ± 0.64	6.37 ± 0.70
E_1 (eV)	23.0 ± 0.1	22.7 ± 0.05	23.0 ± 0.06	22.9 ± 0.03	23.4 ± 0.10	22.1 ± 0.07	22.3 ± 0.06
A_2 (Mb*eV)	1932 ± 1201	1372 ± 628	2735 ± 814	3994 ± 59	7222 ± 2340	5537 ± 3877	5618 ± 3055
Γ_2 (eV)	33.4 ± 10.7	19.9 ± 6.4	14.1 ± 2.8	15.9 ± 1.7	16.3 ± 3.6	21.8 ± 10.3	16.0 ± 4.7
E_2 (eV)	30.9 ± 5.4	35.1 ± 0.9	32.2 ± 0.4	31.7 ± 0.3	31.7 ± 0.6	32.5 ± 1.2	28.6 ± 0.8
A_3 (Mb*eV)		84 ± 430	345 ± 701	568 ± 171	1310 ± 1650	2939 ± 2218	5899 ± 2490
Γ_3 (eV)		7.4 ± 14.0	17.8 ± 3.7	9.0 ± 1.9	12.9 ± 7.6	16.1 ± 4.6	26.1 ± 4.0
E_3 (eV)		48.2 ± 3.7	45.4 ± 1.1	44.7 ± 0.4	45.7 ± 2.3	45.8 ± 1.4	41.2 ± 2.0

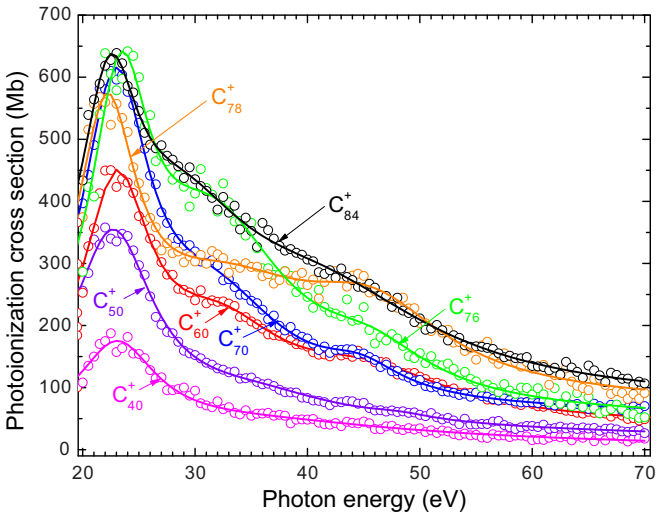

FIG. 4. Comparison of photoionization cross sections for single photoionization of C_n^+ ions on the same scale along with curves representing fits of Eq. (2) to the measurements.

to 22.0 eV reported by Scully *et al.* [6]. This difference is within their combined uncertainties. The variation in the fitted values of the photon energy of the second plasmon is larger, with a mean value of 31.8 ± 1.9 eV. The current value of 32.2 ± 0.4 eV for C_{60}^+ compares to 38 eV reported by Scully *et al.* The weaker harmonic resonance at 45.4 ± 1.1 eV that was unresolved in the measurement of Scully *et al.* likely contributed to the higher value of the fitted energy of the second broad plasmon resonance in their data. In any case, this difference is within the combined uncertainties in the fitting of this broad feature in the two measurements. The mean energy of the third plasmon in the present measurements is 45.1 ± 2.3 eV, which is close to double that of the first plasmon at 22.7 ± 0.4 eV, lending credence to its possible assignment as a harmonic of the surface-plasmon resonance. No evidence for the third plasmon was found in the fitting of the C_{40}^+ data.

Figure 4 presents the measured photoionization cross sections for C_n^+ ions of different n plotted on the same scale along with curves representing the least-squares fits, emphasizing the differences in their magnitudes as well as their dependences on photon energy. Structurally, fullerene molecules have spherical symmetry for $n \leqslant 60$ and become increasingly prolate for higher n, supporting additional modes of oscillation. Their reduced symmetry and the coexistence of different stable structural isomers of the higher-n fullerenes [24,25] may be responsible for the decreasing dominance of the surface-plasmon resonance near 23 eV and a corresponding shift of some of the oscillator strength to higher photon energies. This effect is especially pronounced for C_{78}^+ for which five stable structural isomers have been identified theoretically [26] and detected experimentally [27], consistent with the isolated pentagon rule for fullerenes [28,29]. It is likely that an admixture of structural isomers was present in the C_{78}^+ ion beam but even in this case the energy dependence of the cross section can be accurately represented by Eq. (2).

V. SUMMARY AND CONCLUSIONS

Absolute cross sections were measured in the 18–70 eV photon-energy range for single photoionization of the fullerene molecular ions C_n^+ with $n = 40, 50, 70, 76, 78$, and 84. Oscillator strengths determined by integrating the measured cross sections over this energy range exhibit a linear dependence on the number of carbon atoms, n. For all n, the dominant feature in the cross sections is the strong surface-plasmon resonance near 23 eV previously observed in photoionization of C_{60}, C_{60}^+, and C_{70}. With increasing n there is a shift of oscillator strength to higher photon energies. The cross sections are parametrized by a decreasing linear function of photon energy to represent the small contribution due to direct ionization and three Lorentzian functions centered near 23 eV, 34 eV, and 46 eV to represent plasmon excitations. The third feature found near 46 eV is similar to that previously observed in single photoionization of neutral C_{60} and is attributed to a harmonic of the dominant surface-plasmon resonance.

ACKNOWLEDGMENTS

This research was supported by the Chemical Sciences, Geosciences and Biosciences Division, Office of Basic Energy Sciences, Office of Science, U. S. Department of Energy under Grant No. DE-FG02-03ER15424. Additional funding was provided by the Office of Basic Energy Sciences, U. S. Department of Energy under Contract No. DE-AC03-76SF0098 and by the Deutsche Forschungsgemeinschaft under Grants No. Mu 1068/10 and No. Mu 1068/22. We are grateful to the late L. Dunsch for providing a purified C_{84} sample. The Advanced Light Source is supported by the Director, Office of Science, Office of Basic Energy Sciences, of the U.S. Department of Energy under Contract No. DE-AC02-05CH11231.

[1] H. W. Kroto, J. R. Heath, S. C. O'Brien, R. F. Curl, and R. E. Smalley, Nature (London) **318**, 162 (1985).
[2] E. B. Campbell and F. Rohmund, Rep. Prog. Phys. **63**, 1061 (2000).
[3] F. Lépine, J. Phys. B **48**, 122002 (2015).
[4] G. F. Bertsch, A. Bulgac, D. Tománek, and Y. Wang, Phys. Rev. Lett. **67**, 2690 (1991).
[5] I. V. Hertel, H. Steger, J. de Vries, B. Weisser, C. Menzel, B. Kamke, and W. Kamke, Phys. Rev. Lett. **68**, 784 (1992).
[6] S. W. J. Scully, E. D. Emmons, M. F. Gharaibeh, R. A. Phaneuf, A. L. D. Kilcoyne, A. S. Schlachter, S. Schippers, A. Müller, H. S. Chakraborty, M. E. Madjet, and J. M. Rost, Phys. Rev. Lett. **94**, 065503 (2005).
[7] A. V. Korol and A. V. Solov'yov, Phys. Rev. Lett. **98**, 179601 (2007).
[8] S. W. J. Scully, E. D. Emmons, M. F. Gharaibeh, R. A. Phaneuf, A. L. D. Kilcoyne, A. S. Schlachter, S. Schippers, A. Müller, H. S. Chakraborty, M. E. Madjet, and J. M. Rost, Phys. Rev. Lett. **98**, 179602 (2007).
[9] R. A. Phaneuf, in *Handbook of Nanophysics*, edited by K. D. Sattler (CRC Press, Taylor & Francis Group, London, 2011), Vol. 2, pp. 35-1–35-11.

[10] K. Hansen, R. Richter, M. Alagia, S. Stranges, L. Schio, P. Salén, V. Yatsyna, R. Feifel, and V. Zhaunerchyk, Phys. Rev. Lett. **118**, 103001 (2017).
[11] L. Becker, R. J. Poreda, and T. E. Bunch, Proc. Natl. Acad. Sci. USA **97**, 2979 (2000).
[12] L. Becker, R. J. Poreda, A. G. Hunt, T. E. Bunch, and M. Rampino, Science **291**, 1530 (2001).
[13] K. K. Baral, N. B. Aryal, D. A. Esteves-Macaluso, C. M. Thomas, J. Hellhund, R. Lomsadze, A. L. D. Kilcoyne, A. Müller, S. Schippers, and R. A. Phaneuf, Phys. Rev. A **93**, 033401 (2016).
[14] S. Wang, Phys. Rev. A **60**, 262 (1999).
[15] S. Douix, D. Duflot, D. Cubaynes, J.-M. Bizau, and A. Giuliani, J. Phys. Chem. Lett. **8**, 7 (2017).
[16] A. M. Covington, A. Aguilar, I. R. Covington, M. F. Gharaibeh, G. Hinojosa, C. A. Shirley, R. A. Phaneuf, I. Álvarez, C. Cisneros, I. Dominguez-Lopez, M. M. Sant'Anna, A. S. Schlachter, B. M. McLaughlin, and A. Dalgarno, Phys. Rev. A **66**, 062710 (2002).
[17] G. A. Alna'Washi, M. Lu, M. Habibi, R. A. Phaneuf, A. L. D. Kilcoyne, A. S. Schlachter, C. Cisneros, and B. M. McLaughlin, Phys. Rev. A **81**, 053416 (2010).
[18] F. Broetz, R. Trassl, R. W. McCullough, W. Arnold, and E. Salzborn, Phys. Scr. **T92**, 278 (2001).
[19] K. Rinn, A. Müller, H. Eichenauer, and E. Salzborn, Phys. Sci. Instrum. **53**, 829 (1982).
[20] A. Müller, S. Schippers, J. Hellhund, K. Holste, A. L. D. Kilcoyne, R. A. Phaneuf, C. P. Ballance, and B. M. McLaughlin, J. Phys. B **48**, 235203 (2015).
[21] J. Kou, T. Mori, M. Ono, Y. Harayuma, Y. Kubozono, and K. Mitsuke, Chem. Phys. Lett. **374**, 1 (2003).
[22] J. Kou, T. Mori, S. V. K. Kumar, Y. Harayuma, Y. Kubozono, and K. Mitsuke, J. Chem. Phys. **120**, 6005 (2004).
[23] B. P. Kafle, H. Katayanagi, M. S. I. Prodhan, H. Yagi, C. Huang, and K. Mitsuke, J. Phys. Soc. Jpn. **77**, 014302 (2008).
[24] H. Yang, B. Q. Mercado, H. Jin, Z. Wang, A. Jiang, Z. Liu, C. M. Beavers, M. M. Olmstead, and A. L. Balch, Chem. Commun. **47**, 2068 (2011).
[25] C. Thilgen and F. Diederich, Chem. Rev. **106**, 5049 (2006).
[26] R. D. Bendale and M. C. Zerner, J. Phys. Chem. **99**, 13830 (1995).
[27] K. S. Simeonov, K. Yu. Amsharov, E. Krokos, and M. Jansen, Angew. Chem., Int. Ed. Engl. **47**, 6283 (2008).
[28] H. W. Kroto, Nature (London) **329**, 529 (1987).
[29] P. W. Fowler and D. E. Manolopoulos, *An Atlas of Fullerenes* (Clarendon, Oxford, 2005).